International Symposium
On Turbulence and Shear Flow
Phenomena (TSFP-8)
August 28 - 30, 2013 Poitiers, France

TURBULENCE CONTROL BY INDUCED SPANWISE REFLECTION SYMMETRY BREAKING

George Khujadze
Universität Siegen,
Chair of Fluid Mechanics
Paul-Bonatz-Str. 9-11, 57068 Siegen, Germany
& Abastumani Astrophysical Observatory
Ilia State University, Tbilisi 0160, Georgia
e-mail: george.khujadze@uni-siegen.de

George Chagelishvili
Abastumani Astrophysical Observatory
Ilia State University
& Nodia Institute of Geophysics
Tbilisi State University
Tbilisi, 0160, Georgia
e-mail: g.chagelishvili@astro-ge.org

Martin Oberlack
Chair of Fluid Dynamics
Technische Universität Darmstadt
& Graduate School of Computer Engineering
Technische Universität Darmstadt
Darmstadt 64287, Germany
e-mail: oberlack@fdy.tu-darmstadt.de

ABSTRACT

We propose a new strategy of shear flow turbulence control which is realized by the imposition in the plane Couette flow of a specially designed, non-symmetric in spanwise direction seed velocity perturbations by a near wall volume forcing. The configuration of the imposed perturbations ensures a gain of shear flow energy and the breaking of turbulence spanwise reflection symmetry – generates spanwise mean flow. The latter changes the self-sustained dynamics of turbulence and results in considerable reduction of its level and kinetic energy production. It has to emphasized that the generated spanwise mean flow is a result of the *intrinsic, nonlinear processes* in the forced turbulence and not directly introduced in the system. A model, near-wall weak forcing is designed to impose in the flow the perturbations with required statistics and characteristics. The efficiency of the proposed scheme has been demonstrated by direct numerical simulation (DNS) using the plane Couette flow as a representative example. However, the strategy can be naturally applied to channel and boundary layer flows. The results are promising: the reduction of level of turbulence about 35% was obtained. Of course, the considered forcing is volume and hypothetical one. Nevertheless, it helps to gain a knowledge about the design of the seed velocity field that is necessary to impose in the flow to achieve a substantial reduction of the turbulent kinetic energy.

INTRODUCTION

Control of wall-bounded turbulent flows is an important topic in modern fluid mechanics. Investigations of problems concerned with a reduction of consumption of fuel in aeronautical applications, or reduction of energetic costs at pipeline transportation of fluids, have a century long history. A wide variety of active and passive, linear and nonlinear flow control mechanisms have been suggested and developed over the years. Comprehensive review and analysis of the problem can be found in the following publications (Choi *et al.*, 1993; Gad-el-Hak, 2000; Bewley, 2001; Kim, 2003; Dean & Bhushan, 2010). The fresh discussion of the subject is presented in 2011 year April issue of Phil. Trans. R. Soc. A, on the theme: “Flow-control approaches to drag reduction in aerodynamics: progress and prospects”.

It is now well recognized that the coherent structures play an important role in wall-layer dynamics in turbulent flows (Robinson, 1991). There is strong evidence (see e.g., Kim (2011); Garcia-Mayoral & Jimenez (2011) and references therein) that the most high skin-friction regions in near-wall turbulent layers are induced by the nearby streamwise vortices. The ubiquitous structural features in the near-wall region are streaks, spanwise modulation of the streamwise velocity. *Common features of all drag-reduced flows are weakened near-wall coherent structures.* Generally, streamwise vortices are formed and maintained by a self-sustained dynamics of turbulence, which also involves wall-layer streaks and streamwise-dependent disturbances and is driven by the linear and nonlinear processes associated with these structures.

Recently efforts have been made to control turbulence through the different spanwise wall-based forcing methods (Karniadakis & Choi, 2003). To modify the near-wall turbulence by direct generation of a spanwise mean flow has been tried. There are many different ways of transverse flow generation or modification, e.g. by using the simplified experimental and numerical models of the shark-skin riblets (Garcia-Mayoral & Jimenez, 2011; Goldstein *et al.*, 1995; Strand & Goldstein, 2011), wall oscillations (Ricco *et al.*, 2012; Touber & Leschziner, 2012) and streamwise traveling waves (Quadrio *et al.*, 2009). However, there could be another, indirect way of a spanwise mean flow generation,

for instance, by a week near-wall forcing that initiates the breaking of turbulence spanwise reflection symmetry that, in turn, leads to the turbulence control. The scheme of this control strategy is the following:
(i) a specially designed (non-symmetric in spanwise direction) near-wall weak volume forcing generates seed velocity perturbations that draw the shear flow energy and undergo substantial transient growth;
(ii) the amplified non-symmetric velocity perturbations lead to the breaking of turbulence reflection symmetry and the generation of mean spanwise flow;
(iii) the latter, in turn, changes the statistics of the turbulence leading to a considerable reduction of its level.

NON-SYMMETRIC NEAR-WALL FORCING

We consider forced incompressible plane Couette flow with shear parameter A and Reynolds number $Re \equiv UL/\nu = AL^2/\nu$, based on the wall velocity U, the channel half-width L, and the kinematic viscosity ν. We use (x,y,z) for the streamwise, wall-normal and spanwise directions respectively. No-slip boundary conditions are used on the walls.
The transient growth of perturbations due to the non-normality of the linearized dynamical operators of shear flow is the basis of the dynamical activity in smooth shear flows. It is well-known that the constant shear flows for sufficiently high Reynolds numbers support a set of optimal perturbations that undergo large transient growth during the dynamical time of turbulence. The latter can be defined as the characteristic time of the nonlinear processes $\mathcal{O}(1/A)$. A robust growth takes place for $3D$ perturbations that satisfy the following conditions:
– characteristic streamwise and spanwise scales are the same order and at the same time both are larger than the viscous dissipative length scale, $\ell_x \simeq \ell_z \gg \ell_\nu$, or, in terms of wavenumbers, $k_x, k_z \ll k_\nu$ (here, $k_\nu \equiv \sqrt{Re} \approx 1/\ell_\nu$);
– the perturbations are tilted with the background shear (Craik & Criminale, 1986; Farrell & Ioannou, 1993), or, in terms of wavenumbers, $k_y/k_x < 0$.
This type of seed (i.e., small amplitude) velocity perturbations can be imposed in the flow by the following model of the helical forcing (see Figure 1):

$$
\begin{aligned}
F_x(x,y,z) =& A_1 \cdot \sin(\pi y) \cdot \exp\left[-\frac{(|y|-y_{peak})^2}{l_y^2}\right] \\
&\times \sum_{n,m=0}^{N,M} Z_m \cdot \exp\left(-X_n^2 - Z_m^2\right) \exp\left(-\frac{\hat{X}_n^2}{l_x^2} - \frac{\hat{Z}_m^2}{l_z^2}\right) \\
F_y(x,y,z) =& -A_2 \cdot \sin(\pi y) \cdot \exp\left[-\frac{(|y|-y_{peak})^2}{l_y^2}\right] \\
&\times \sum_{n,m=0}^{N,M} \exp\left(-X_n^2 - Z_m^2\right) \exp\left(-\frac{\hat{X}_n^2}{l_x^2} - \frac{\hat{Z}_m^2}{l_z^2}\right) \\
F_z(x,y,z) =& -A_1 \cdot \sin(\pi y) \cdot \exp\left[-\frac{(|y|-y_{peak})^2}{l_y^2}\right] \\
&\times \sum_{n,m=0}^{N,M} X_n \cdot \exp\left(-X_n^2 - Z_m^2\right) \exp\left(-\frac{\hat{X}_n^2}{l_x^2} - \frac{\hat{Z}_m^2}{l_z^2}\right)
\end{aligned}
\tag{1}
$$

where $f(y) = \sin(\pi y) \exp\left[-\frac{(|y|-y_{peak})^2}{l_y^2}\right]$, $y \in [-1,1]$
$X_n, Z_m, \hat{X}, \hat{Z}$ on the bottom wall ($y=-1$):

$$
\begin{aligned}
X_n(a,\phi) =& \frac{x}{a} - 2n\cos\phi, \\
Z_m(a,\phi) =& \frac{z}{a} - 1 - (4m+1)(1-\sin\phi) \\
\hat{X}_n(a,\phi) =& \frac{x}{a} - (2n+1)\cos\phi \\
\hat{Z}_m(a,\phi) =& \frac{z}{a} - (4m+2)(1-\sin\phi)
\end{aligned}
\tag{2}
$$

$X_n, Z_m, \hat{X}, \hat{Z}$ on the top wall ($y=1$):

$$
\begin{aligned}
X_n(a,\phi) =& \frac{L_x - x}{a} - 2n\cos\phi \\
Z_m(a,\phi) =& \frac{L_z - z}{a} - 1 - (4m+1)(1-\sin\phi) \\
\hat{X}_n(a,\phi) =& \frac{L_x - x}{a} - (2n+1)\cos\phi \\
\hat{Z}_m(a,\phi) =& \frac{L_z - z}{a} - (4m+2)(1-\sin\phi)
\end{aligned}
\tag{3}
$$

where $L_x = 2a(N-1)\cos\phi$ and $L_z = 4aM(1-\sin\phi)$ are sizes of the simulation box and $N+1$ and $M+1$ are numbers of the forcing centers in the streamwise and spanwise directions, respectively; a and ϕ define the configuration of the forcing (a defines the forcing "cells" size and ϕ – the forcing orientation in $x-z$ plane, e.g., at $\phi = \pi/4$ quasi equipartition of the forcing in the streamwise and spanwise directions occurs); l_x, l_y and l_z are sizes of the forcing localizations in the streamwise, wall-normal and spanwise directions; A_1 and A_2 define the forcing amplitudes in the streamwise/spanwise and wall-normal directions; $X_n(a,\phi)$ and $Z_m(a,\phi)$ define the location of the forcing symmetry centers and $\hat{X}_n(a,\phi)$ and $\hat{Z}_m(a,\phi)$ define the location of the forcing localization centers in the streamwise and spanwise directions, respectively; y_{peak} defines the location of the forcing localization center in the wall-normal direction.

RESULTS OF NUMERICAL SIMULATIONS

The pseudo-spectral code developed at KTH, Stockholm was used in the simulations. Fourier decomposition in the horizontal (x and z) and Chebyshev discretization in the wall-normal (y) directions were used respectively. Time integration was performed using a third-order Runge-Kutta method for the advective and forcing terms and Crank-Nicolson for the viscous terms. All quantities were normalized on the half of the velocity difference between the walls and the channel half-width (for details see Skote (2001)). The original code was modified to implement the forcing presented by Eqs.1. DNS at different parameters of the controlled and unmanipulated flows have been performed at $Re = 750$. (The turbulent Reynolds number based on friction velocity and channel half-width was $Re_\tau = 52$.) The simulation box was $L_x \times L_y \times L_z = 8\pi \times 2 \times 4\pi$. Two different number of modes were used $N_x \times N_y \times N_z = 256 \times 97 \times 128$, $512 \times 257 \times 256$ to study the grid convergence. The simulations have shown that the increase of number of modes does not change the numerical results. The resolution of the simulations was $\Delta x^+ = 5$, $\Delta y^+ = 0.03 - 1.6$, $\Delta z^+ = 5$. The statistics and instantaneous velocity fields of the unmanipulated and forced

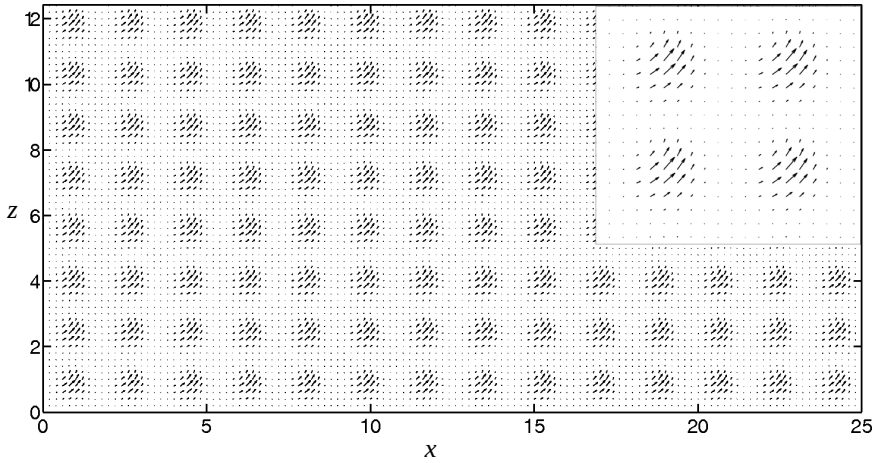

Figure 1. Geometry of the forcing with a zoomed segment in the plane $y = -y_{peak} = -095$ with parameters: $N = 13, M = 7, a = 1.2221, \phi = \pi/4, l_x = l_z = 1/\sqrt{10}, l_y = 0.2, A_1 = 0.4, A_2 = 0.008$.

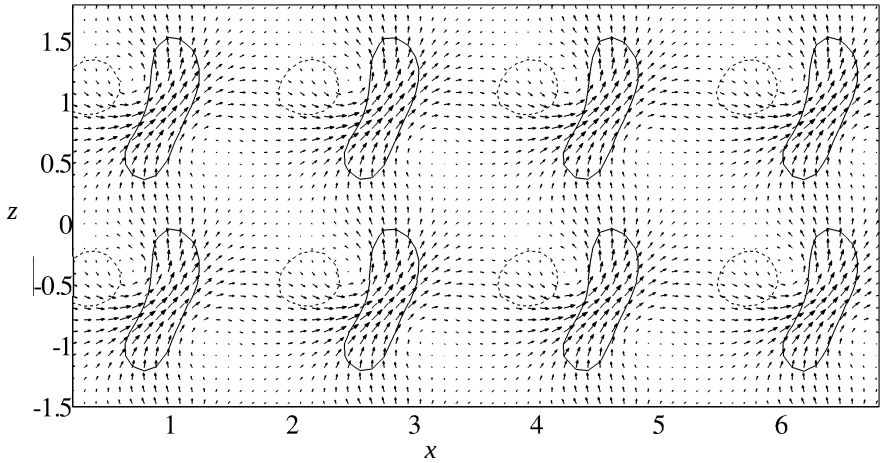

Figure 2. Velocity field imposed by the forcing in xz-plane at $y = -y_{\text{peak}} = -0.95$ with contours of positive (0.0005 ——) and negative (-0.0001 – – –) spanwise velocity.

turbulence were compared. It was found that the production of turbulent kinetic energy is very sensitive to the forcing parameters. Here only the case with the significant reduction of turbulent kinetic energy production is presented.

Figure 2 presents the imposed at each action of the forcing the seed velocity field in the xz-plane $y = -0.95$ and contours 0.0005 (solid line) and -0.0001 (dashed line) of the spanwise velocity component. The vector field in the area of the solid contour initiates the breaking of the spanwise symmetry. The velocity field in the area of the dashed contour is due to the incompressibility condition and is unfavorable to the spanwise symmetry breaking. Nevertheless, the imposed velocity configuration, for the set of parameters presented in Figure 1 leads to the generation of mean spanwise velocity and, finally, to substantial reduction of the turbulent kinetic energy.

It is well known that Couette flow is spectrally stable and that the turbulence in this flow has a subcritical nature which is realized by the bypass concept. The proposed strategy or route of the flow control is based on peculiarities of linear and nonlinear processes in the framework of the bypass concept, according which the self-sustenance of the turbulence in shear flows is the result of the linear transient growth of kinetic energy of perturbations induced by the non-normality of these flows and positive nonlinear feedback. The role of nonlinearity in this case is principally different from the role in the Kolmogorov theory. The turbulence level/balance depends on the nonlinear redistribution process in the wavenumber space. If we act somehow on the nonlinear redistribution process, the balance between the linear and nonlinear processes can be achieved at different levels (low or high) of turbulence. So, at the control the imposed specially designed perturbations after transient growth become powerful and active participant of the nonlinear redistribution process, change it and lead to the balance at a lower level of turbulence. In Figure 3 the slices of the spanwise velocity for the unmanipulated (top plot) and controlled (bottom plot) flows are shown in xy plane. The levels of contours are in the range of $[-0.3, 0.3]$. Green and red colors correspond to the negative and positive spanwise velocities correspondingly. In the case of unmanipulated turbulent flow, the contours with different signs are uniformly distributed in the wall-normal direction that give, as it was expected, zero mean spanwise flow. A completely different picture is observed on the bottom plot, for the controlled flow. The contours with the negative values are mainly located in the upper half of the simulation box and the contours with the positive values are in the lower half of it. This means the appearance and generation of the mean flow in the spanwise direction. The another feature of the controlled flow is also observed. The coherent structures in the flow become rare indicating a reduction of the level

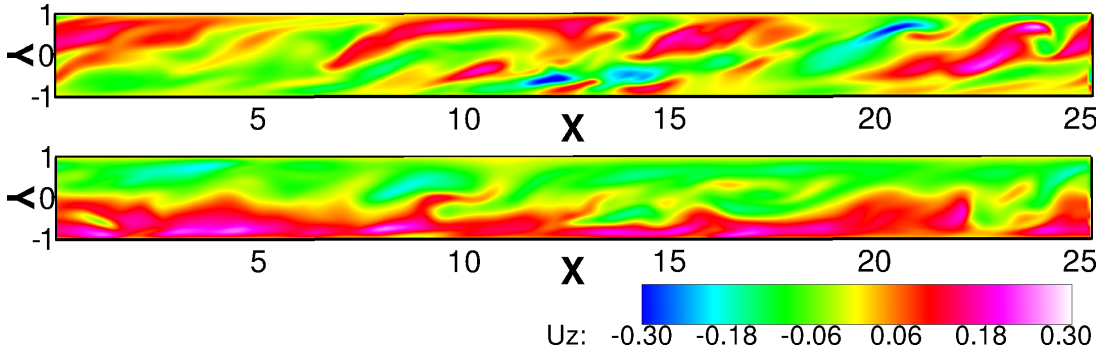

Figure 3. Slices of spanwise velocity in *xy*-plane for unmanipulated (top plot) and controlled (bottom plot) flows.

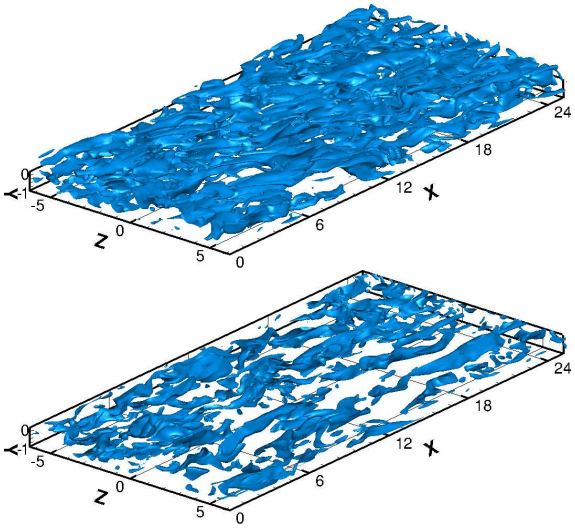

Figure 4. Iso-surfaces of streamwise of vorticity ($\omega_x = 0.5$) at lower wall for turbulent (top plot) and controlled (bottom) flows. The coherent structures in the controlled flow become rare that indicates a reduction of level of turbulence.

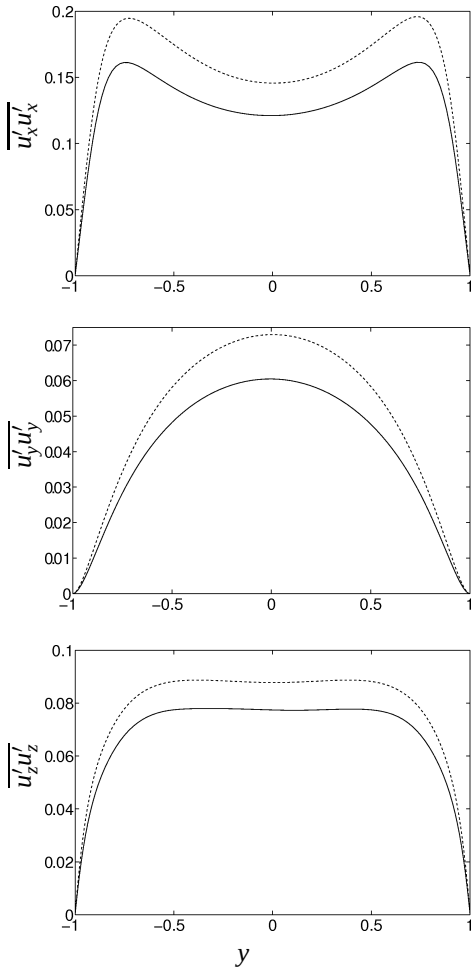

Figure 5. Diagonal components of Reynolds stress tensor for unmanipulated turbulent (- - -) and controlled (——) flows.

of the turbulence intensity that one can see from the plots in Figure 4 which presents iso-surfaces of streamwise component of vorticity (ω_x) for turbulent (top plot) and controlled (bottom plot) at the lower wall. The statistics of Reynolds stress tensor components in unmanipulated (dashed lines) and forced, controlled (solid lines) cases are shown in Figures 5, 6 and 7. The plots in Figure 7 represents the non-diagonal components of Reynolds stress tensor that usually are zero in the unmanipulated flow, they appear only in the controlled flow. The plots of Reynolds stress components show that the level of turbulence decreases significantly in the latter case. Figures 8 and 9 show the deviation of the controlled flow mean streamwise ($\Delta\overline{U}_x = \overline{U}_x^{contr} - \overline{U}_x^{turb}$) and spanwise ($\Delta\overline{U}_z = \overline{U}_z^{contr} - \overline{U}_z^{turb}$) velocity profiles from the unmanipulated flow corresponding profiles. It is obvious that the forcing does not create the mean wall-normal flow. The left plot shows that the maximum deviation of the controlled flow mean streamwise velocity is quite small: $\Delta\overline{U}_{x,max} \approx 0.014$. For the unmanipulated turbulent flow, the mean spanwise velocity is zero, consequently, $\Delta\overline{U}_z = \overline{U}_z^{contr}$. For the controlled flow the mean spanwise velocity appears with the maximum value $\overline{U}_{z,max}^{contr} \approx 0.07$.

As for the production of turbulent kinetic energy, besides the classical term, $Pr_x = -\overline{u'_x u'_y} d\overline{U}_x/dy$, the additional component, $Pr_z = -\overline{u'_y u'_z} d\overline{U}_z/dy$, appears due to the forcing. The power input in the flow can be defined by: $P^{in} = \overline{F_x u'_x} + \overline{F_y u'_y} + \overline{F_z u'_z} \equiv P_x^{in} + P_y^{in} + P_z^{in}$, where the term P_y^{in} is negligible. The terms characterizing the energetics of the control process (as a function of wall-normal coordinate) are presented in Figure 10. The top plot displays P_x^{in} (dashed-dotted line) and Pr_x for the unmanipulated (dashed line) and controlled (solid line) flows. The bottom plot displays the same but for the spanwise components. These figures show that $P_x^{in}, P_z^{in}, Pr_z \ll Pr_x$ and the turbulent kinetic energy production is substantially reduced in the controlled case.

The results presented in Figure 10 are confirmed by plots in Figures 11 and 12 that displays the time evolution of the (averaged in the streamwise, wall-normal and span-

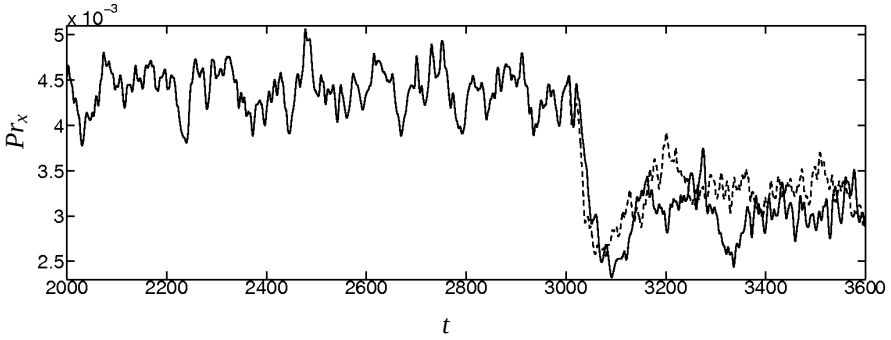

Figure 11. Time evolution of the production of turbulent kinetic energy (averaged in space) for the unmanipulated ($t < 3000$) and controlled ($t > 3000$) flows at two different locations of the forcing centers in the wall-normal direction: $y_{peak} = 0.95$, ——, and $y_{peak} = 0.90$, - - -.

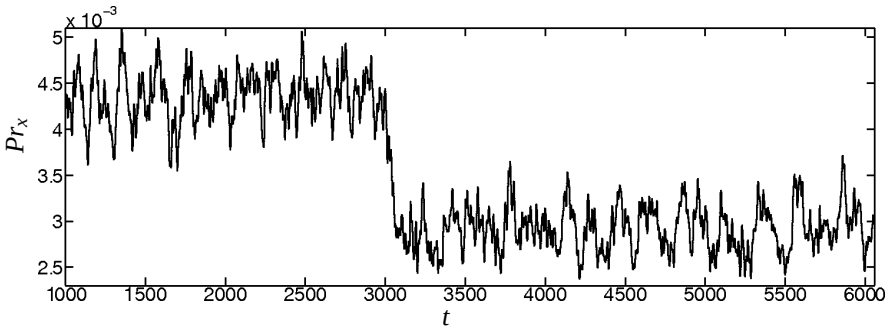

Figure 12. Time evolution of the production of turbulent kinetic energy for unmanipulated ($t < 3000$) and controlled ($t > 3000$) flows for $y_{peak} = 0.95$.

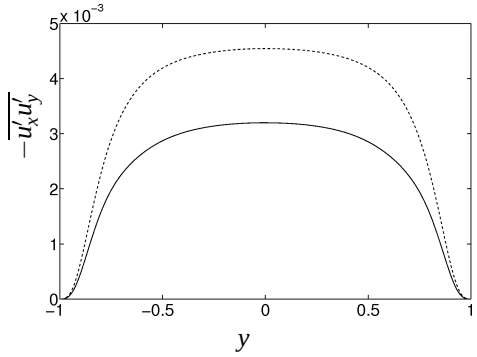

Figure 6. $\overline{u'_x u'_y}$ component of Reynolds stress tensor for unmanipulated turbulent (- - -) and controlled (——) flows.

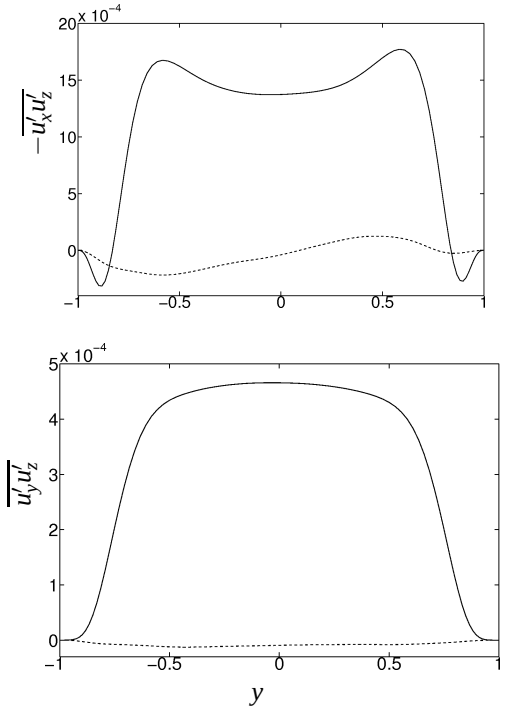

Figure 7. $\overline{u'_y u'_z}$ and $\overline{u'_x u'_z}$ components of Reynolds stress tensor for unmanipulated turbulent (- - -) and controlled (——) flows.

wise directions) production of turbulent kinetic energy. The time region $t \leq 3000$ corresponds to the unmanipulated turbulent flow and $t > 3000$ corresponds to the manipulated and controlled flow. As a result, the reduction of the level of turbulence about 35% was obtained. Figure 11 compares the time evolutions of the productions for two different locations of the forcing center in the wall-normal direction. The figure shows that the shifting of the forcing location away from the wall (from $y_{peak} = 0.95$ to $y_{peak} = 0.90$) remarkably changes (in the worse direction) the reduction of turbulent kinetic energy production. In Figure 12 the longer time evolution of Pr_x in the case of forcing for $y_{peak} = 0.95$ is presented.

CONCLUSIONS

The aim of this study was to propose and analyse a new strategy/route of the flow control by imposition in the flow a specially designed seed perturbations with the special length scales that have potential of transient growth. These perturbations generate the helical turbulence (that has nonzero streamwise vorticity) and simultaneously create the spanwise mean flow.

Taking into account the feature of the subcritical turbulence and definition of optimal perturbations the model of near-wall body forcing with nonzero helicity was con-

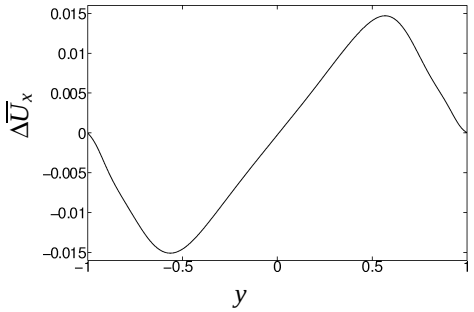

Figure 8. The deviation of the controlled flow mean streamwise ($\Delta\overline{U}_x$) velocity profile from the unmanipulated turbulent flow.

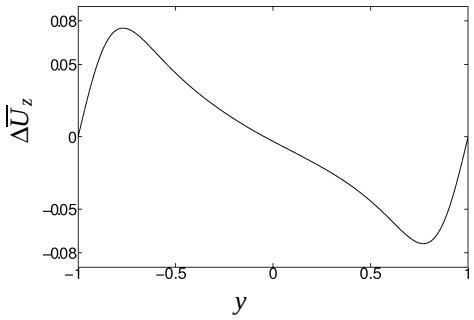

Figure 9. The deviation of the controlled flow mean spanwise ($\Delta\overline{U}_z$) velocity profile from the unmanipulated turbulent flow.

structed and DNS was performed to evaluate the efficiency of the proposed scheme on the example of plane Couette flow. The results are promising and encouraging: the applied forcing considerably reduces the kinetic energy production in comparison to the unmanipulated turbulent flow. Of course, the considered forcing is volume and hypothetical one. However, the forcing helps to gain the knowledge about the design of the seed velocity field, permanent (at each simulation time step) imposing of which leads to the substantial reduction of the turbulent kinetic energy. This convinces in the vitality of the proposed control strategy and initiates further investigations. It is obvious that the imposition of the needed seed perturbations can be achieved by manipulation of the boundary conditions. Specifically, by the properly designed blowing and suction or riblets. To design the nonuniform blowing and suction and study the flow control is the next step of our activity. As for the riblets that replicate the shape of the shark-skin, their design can be quite complicated that is the final aim of our investigation.

of three-dimensional perturbations in viscous constant

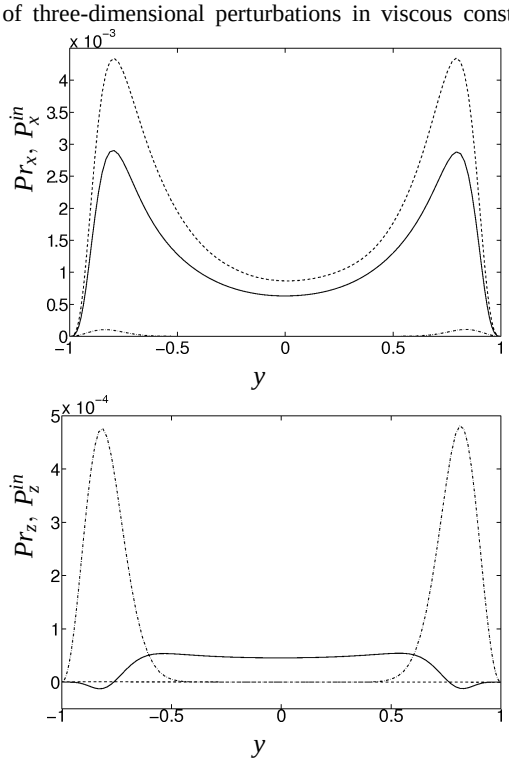

Figure 10. Top plot: Time averaged streamwise component of turbulent kinetic energy production, Pr_x, for the unmanipulated turbulent (– – –) and controlled (——) flows and input power, P_x^{in}, (—·—); Middle plot: The same for the spanwise components.

REFERENCES

Bewley, T. R. 2001 Flow control: new challenges for a new renaissance. *Progress in Aerospace Sciences* **37**, 21–53.

Choi, H., Moin, P. & Kim, J. 1993 Direct numerical simulation of turbulent flow over riblets. *J. Fluid Mech.* **255**, 503–539.

Craik, A. D. D. & Criminale, W. O. 1986 Evolution of Wavelike Disturbances in Shear Flows: A Class of Exact Solutions of the Navier-Stokes Equations. *Proc. R. Soc. Lond. A* **406**, 13–26.

Dean, B. & Bhushan, B. 2010 Shark-skin surfaces for fluid-drag reduction in turbulent flow: A review. *Phil. Trans. R.Soc.A* **368** (4775-4806).

Farrell, B. F. & Ioannou, P. J. 1993 Optimal excitation of three-dimensional perturbations in viscous constant shear flow. *Phys. Fluids A* **5**, 1390–1400.

Gad-el-Hak, M. 2000 *Passive, Active and Reactive Flow*. Cambridge, UK: Cambridge Univ. Press.

Garcia-Mayoral, R. & Jimenez, J. 2011 Hydrodynamic stability and breakdown of the viscous regime over riblets. *J. Fluid Mech.* **678**, 317–347.

Goldstein, D., Handler, R. & Sirovich, L. 1995 Direct numerical simulation of turbulent flow over a modelled riblet covered surface. *J. Fluid Mech.* **302**, 333–376.

Karniadakis, G. E. & Choi, K.-S. 2003 Mechanisms on transverse motions in turbulent wall flows. *Annu Rev. Fluid Mech.* **35**, 45–62.

Kim, J. 2003 Control of turbulent boundary layers. *Physics of Fluids* **15**, 1093–1105.

Kim, J. 2011 Physics and control of wall turbulence for drag reduction. *Phil. Trans. R. Soc. A* **369**, 13961411.

Quadrio, M., Ricco, P. & Viotti, C. 2009 Streamwise-travelling waves of spanwise wall velocity for turbulent drag reduction. *J. Fluid Mech.* **627**, 161–178.

Ricco, P., Ottoneli, C., Hasegawa, Y. & Quadrio, M. 2012 Changes in turbulent dissipation in a channel flow with oscillating walls. *J. Fluid Mech.* **700**, 77–104.

Robinson, S. K. 1991 Coherent motions in the turbulent boundary layer. *Annual Review of Fluid Mechanics* **23**, 601–639.

Skote, M. 2001 Studies of turbulent boundary layer flow through direct numerical simulation. PhD thesis, Royal Institute of Technology,Stockholm, Sweden.

Strand, J.S. & Goldstein, D.B. 2011 Direct numerical simulations of riblets to constrain the growth of turbulent spots. *J. Fluid Mech.* **668**, 267–292.

Touber, E. & Leschziner, M.A. 2012 Near-wall streak modification by spanwise osscilatory wall motion and drag-reduction mechanisms. *J. Fluid Mech.* **693**, 150–200.